Nonlinear Evolution of Collisionless Electron Beam–Plasma Systems

JAMES R. THOMPSON*,†
Department of Physics, University of Texas at Austin, Austin, Texas 78712

(Received 6 August 1970; final manuscript received 3 March 1971)

The problem of the nonlinear time evolution of a cold beam–plasma system, for which weak turbulence theory is well known to be inapplicable, is examined under the restrictions to one-dimensional electrostatic oscillations and for systems where the ratio of the beam density to the background plasma density is a small parameter. In this case, it may be shown that the electrostatic field undergoes rapid growth to a state of meta-equilibrium, followed by a slower time development. The mechanism for the nonlinear saturation of this growth is the trapping of beam electrons in the wave troughs of the electrostatic field. The existence of a unique single wave nonlinear Bernstein–Greene–Kruskal stationary state is established for this system and its properties (e.g., its energy content, wavelength, phase velocity) are evaluated. This Bernstein–Greene–Kruskal state is apparently approached closely by the system in the course of its time evolution. The predictions of the theories are compared with computer calculations and are found to be in good agreement.

I. INTRODUCTION

The problem considered herein is the nonlinear behavior of unstable collisionless cold beam–plasma systems. Most successful advances of nonlinear plasma theory have fallen within the framework of "weak turbulence," introduced by the 1962 treatment of the "gentle bump" instability by Drummond and Pines,[1] and by Vedenov, Velikhov, and Sagdeev.[2] This weak turbulence theory is characterized by an expansion of perturbations on the Maxwell–Vlasov equations in powers of the electric field energy, typically yielding a wave kinetic equation (for the time evolution of the spectrum) which may be cast in a quantum mechanical vernacular a la Feynman.[3] Although this weak turbulence theory may be applied to a large class of plasma instabilities, including the gentle bump instability mentioned above, the requirements for its validity are violated for many other instabilities, among which is the cold (hence not gentle) beam–plasma instability. However, the increasing study of such problems through numerical simulation on high-speed digital computers[4,5] provides considerable guidance for the development of a new theory.

Among the restrictions which underlie this analysis are the assumption of a spatially homogeneous initial state, the neglect of ion dynamics[6] (formally by assuming an infinite ion mass), the restriction to one spatial dimension (although physical relevance may be retained for systems in which an "infinite" magnetic field likewise restricts the particle motion to one dimension), the neglect of all effects associated with finite static magnetic fields, and the imposition of periodic boundary conditions in space with an initial value problem posed in time.

In addition, the following ordering of lengths is assumed, as discussed also by Buneman,[7] to justify further simplifications which are itemized below:

$$D > 2\pi c/\omega_{pe} \gg 2\pi u/\omega_{pe} \gg \lambda_{De} \gg d, \tag{1}$$

where D is a characteristic plasma dimension, c is the speed of light, u is the streaming velocity of the beam with respect to the background plasma, $\omega_{pe} \equiv (4\pi ne^2/m)^{1/2}$ is the electron plasma frequency, $\lambda_{De} \equiv (T/4\pi ne^2)^{1/2}$ is the Debye shielding distance, d is the average interparticle distance, and $e(=|e|)$, m, n, and T are the electronic charge, mass, density, and temperature in energy units, respectively.

(a) Surface or boundary effects are neglected.

(b) Relativistic effects are neglected, and only longitudinal electrostatic oscillations are considered. Hence, the electric field E may be represented as the gradient of an electrostatic potential φ: $E = -\partial\varphi/\partial x$.

(c) The initial state of the system is assumed to consist of two species of *cold* electrons (background electrons and beam electrons), and we are particularly interested in the case where the relative streaming velocity u between these two species is orders of magnitude larger than the thermal velocity $(T/m)^{1/2}$ of either species, so that the initial velocity distribution may be adequately represented by a delta function.

(d) The plasmas are assumed to be collisionless, and hence dominated by collective effects.

Finally, the density of the beam electrons is assumed to be much less than that of the background electrons, so that $\eta \equiv (\omega_{pb}^2/\omega_{pe}^2) \ll 1$ is a small parameter. In fact, we shall strengthen this assumption by also requiring that $\eta^{1/3} \ll 1$ since it is this latter quantity which appears in many of the expansions. Corollaries of this assumption are the dominance of the electrostatic field spectrum by a single Fourier mode, and the existence of an adiabatic invariant to describe the evolution of the background electrons in the (x, v) phase space.

The basic equations for the problem are the Vlasov equation for the distribution function of each particle species, and Poisson's equation for the self-consistent electric field. These equations and all of their consequences are invariant under Galilean transformations.

From the Vlasov–Poisson equations and the assumption of periodic boundary conditions, the usual conservation equations follow immediately:

$$\frac{d}{dt}\langle n_j(x,t)\rangle = \frac{d}{dt}\left\langle \int_{-\infty}^{\infty} dv F_j(x,v,t)\right\rangle = 0, \quad (2)$$

i.e., particles of each species are conserved;

$$\frac{d}{dt}P(t) = \frac{d}{dt}\sum_{j=e,b} m_j \left\langle \int_{-\infty}^{\infty} dv v F_j(x,v,t)\right\rangle = 0 \quad (3)$$

i.e., the total momentum density is conserved;

$$\frac{d}{dt}[T(t)+\mathcal{E}(t)] = \frac{d}{dt}\left(\sum_{j=e,b}\tfrac{1}{2}m_j\left\langle\int_{-\infty}^{\infty} dv v^2 F_j(x,v,t)\right\rangle + \frac{1}{8\pi}\langle E^2(x,t)\rangle\right) = 0, \quad (4)$$

i.e., the total energy density is conserved. Here, F_j, P, T, and $\mathcal{E}$ are the particle distribution function, momentum density, kinetic energy density, and electric field energy density; the subscripts e and b denote background and beam electrons, respectively; and the symbol $\langle\ \rangle$ denotes a spatial average. Although $\langle n_j(x,t)\rangle$, $\mathcal{E}(t)$, and Eqs. (2), (3), and (4) are frame-independent, $P_j(t)$ and $T_j(t)$ will be frame-dependent.

II. REVIEW OF LINEAR THEORY AND THE INITIAL NONLINEAR DEVELOPMENT

Since the linear theory of beam–plasma systems is well known,[8] and a simple model of the initial nonlinear development of this problem has been presented by Drummond *et al.*,[9] we confine ourselves to the following brief review.

In the laboratory frame, the linear dispersion relation is

$$1-(\omega_p^2/\omega^2)-[\eta\omega_p^2/(\omega-ku)^2]=0, \quad (5)$$

where $\omega_p \equiv \omega_{pe}$, k is taken to be real, and $\omega(k)$ is the complex frequency which describes the time behavior of the kth Fourier mode. The solution to (5) is depicted graphically in Fig. 1, which reveals the existence of complex conjugate unstable solutions for ω when $|k|<(\omega_p/u)(1+\eta^{1/3})^{3/2}$. The frequency, wavenumber growth rate, and group velocity of the most unstable linear wave are

$$\bar{\omega}_L=\omega_p[1-\tfrac{1}{2}(\tfrac{1}{2}\eta)^{1/3}+\tfrac{3}{4}(\tfrac{1}{2}\eta)^{2/3}+\cdots];$$
$$k_L=(\omega_p/u)[1+\tfrac{3}{2}(\tfrac{1}{2}\eta)^{2/3}+\cdots];$$
$$\gamma_L=\omega_p[\tfrac{1}{2}\sqrt{3}(\tfrac{1}{2}\eta)^{1/3}-\tfrac{1}{4}\sqrt{3}(\tfrac{1}{2}\eta)^{2/3}+\cdots]; \quad (6)$$
$$\left(\frac{d\bar{\omega}}{dk}\right)_L=u[\tfrac{2}{3}-\tfrac{1}{3}(\tfrac{1}{2}\eta)^{1/3}+\cdots].$$

The extremely peaked growth rate function $\gamma(k)$ is one of the most striking results of linear theory, since it will produce a very narrow wave spectrum. The half-width of $\gamma(k)$ is $\Delta k=O(\eta^{1/3}k_L)$. Since we have assumed an extremely low initial noise level, the unstable waves must e-fold many times before nonlinear effects become important. After N e-folds (i.e., $N=\gamma_L t$), the half-width of the energy spectrum is $\delta k=O(N^{-1/2}\eta^{1/3}k_L)$ and hence in the limit $\eta^{1/3}\ll 1$ and $N^{1/2}\gg 1$ the wave spectrum may become effectively dominated by a single sinusoidal oscillation.

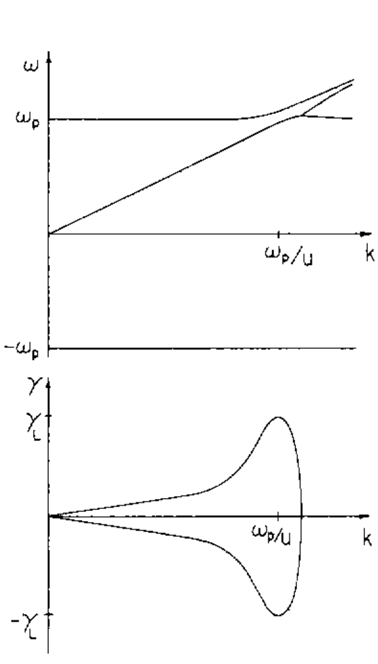

FIG. 1. Linear dispersion relation.

To explore the plausibility of a single wave spectrum somewhat more thoroughly, we consider the normalized autocorrelation function:

$$U(t,\tau)\equiv\langle\langle E^*(x,t)E(x,t+\tau)\rangle\rangle/\langle\langle|E(x,t)|^2\rangle\rangle,$$

where $\langle\langle\ \rangle\rangle$ is a statistical phase averaging operation that may be replaced by a time average by appeal to an ergotic theorem. In linear theory one obtains

$$U(t,\tau)=\sum_{k=-\infty}^{\infty}\frac{\mathcal{E}_k(t)}{\mathcal{E}(t)}\exp[\gamma(k)\tau-i\bar{\omega}(k)\tau], \quad (7)$$

where

$$\mathcal{E}(t)=\sum_{k=-\infty}^{\infty}\mathcal{E}_k(t) = \frac{1}{8\pi}\sum_{k=-\infty}^{\infty}|E_k|^2\exp[2\gamma(k)t]$$

is the linear mode decomposition of the field energy density. In the case of a single (k_1) mode this reduces to $U_{k1}(t,\tau)=\exp[\gamma(k_1)\tau]\cos\bar{\omega}(k_1)\tau$ and except for the ordinary damping or growth evidenced by $\gamma(k_1)$, the single wave autocorrelation function experiences no decay as $\tau\to\infty$ so that a single wave should retain its waveform indefinitely according to linear theory. However, for a spectrum of growing waves, the autocorrelation function reveals two competing effects in addition to the ordinary growth. First, there is the increasing tendency of the various mode contributions to $U(t,\ \tau)$ to cancel with increasing τ causing the eventual decay of the correlation function to zero. This primary effect is only slightly retarded by the tendency of the wave spectrum to narrow as it e-folds with τ. The result, in this case, is the correlation time $\tau_c \approx (2N^{1/2}+1)/\gamma_L$, where $|U(t,\ \tau\geq\tau_c|\leq\frac{1}{2}\exp(\gamma_L\tau)$. Although the correlation time is not infinite as for a single wave, the fact that it is many e-folding periods suggest that the dominance of the wave spectrum by a single mode may persist well into the nonlinear regime. It is this intermediate time, nonlinear single wave regime of the instability which we now consider.

Examination of the single wave linear theory reveals that by the time that the electric field energy density has grown to $\mathcal{E}(t)\approx 0.20\eta^{1/3}T_b(0)$, where $T_b(0)=\frac{1}{2}mn_bu^2$ is the initial kinetic energy density of the beam electrons, the density fluctuations of the beam electrons will have become so large that linear theory is no longer valid for them. However, the background electrons continue to obey linear theory. In addition, because the background electrons have a large velocity relative to the growing wave, one may define for them a quantity $J=\langle|v(H,\ x,\ t)|\rangle$ which is preserved adiabatically invariant during their evolution.

According to this approximation, which is discussed in more detail in the Appendix, the "fast" background electrons "see" the electric field growing so slowly that they cling to phase space trajectories of constant energy. In the wave frame, these have the form

$$H(x,\ v,\ t)=\tfrac{1}{2}mv^2-[eE(t)/k]\cos kx, \qquad (8)$$

where

$$E(x,\ t)=E_0\exp\left(\int_0^t d\tau\ \gamma(\tau)\right)\sin kx=E(t)\ \sin kx$$

is the electric field. These trajectories in turn deform slowly so as to preserve J invariance.

Single particles obey Hamiltonian equations of motion, with H given in Eq. (8). If the time dependence of $E(t)$ were to vanish, H would be a constant of the motion and the constant energy contours of Eq. (8) would be the actual particle trajectories so long as $\dot{E}(t)=0$. When $E(t)$ is weakly time dependent (i.e., its change is small during a particle transit time across a wavelength), H is nonconstant so that the contours deform in phase space according to J invariance.

The function $v(H,\ x,\ t)$ required in the definition of J is obtained by inverting Eq. (8), and H and t are to be held fixed during the spatial average. One finds

$$J=\frac{4}{\pi}\left(\frac{eE(t)}{mk}\right)^{1/2}\{S(\kappa-1)\kappa E_2(\kappa^{-1}) + S(1-\kappa)[E_2(\kappa)-(1-\kappa^2)K(\kappa)]\}, \qquad (9)$$

where $\kappa\equiv\{\frac{1}{2}[1+kH/eE(t)]\}^{1/2}$, K and E_2 are complete elliptic integrals of the first and second kind, and $S(\rho)=\frac{1}{2}+\frac{1}{2}\ \mathrm{sgn}\rho$ is the unit step function.

The constant energy contours of Eq. (8), illustrated by the dashed lines in Figs. 1–3 of Ref. 9, are unbounded in x for $\kappa>1$, but are closed bounded contours for $\kappa<1$. Since $E(t)$ is initially quite small, $\kappa(t)$ is initially quite large, and as $E(t)$ increases $\kappa(t)$ must decrease for J to remain invariant. We call $\kappa(t)$ the trapping parameter; particles for which $\kappa>1$ are said to be untrapped and those for which $\kappa<1$ are said to be trapped. However, it should be clearly noted that a particle which is instantaneously located on a trapped energy contour will move on that contour only if the adiabatic approximation is valid, and even then the contour may slowly deform. Furthermore, it is possible for a particle once located on a trapped contour to subsequently be located on an untrapped contour if the electric field magnitude were to decrease sufficiently.

Since the brace in Eq. (9) is a monotonically increasing function of κ, the adiabatic approximation requires that κ should continually decrease so long as $E(t)$ increases. Hence, there is some critical field amplitude for which κ is reduced to 1 and the particles in question become trapped. This first occurs for particles with the lowest J. The background electrons have $J_e=|v_{0e}|=u-v_{0b}=u[1-O(\eta^{1/3})]$, evaluated initially when $E(0)\approx 0$ and using the linear wave phase velocity. The beam electrons have $J_b=v_{0b}=O(\eta^{1/3}u)\ll J_e$, which correctly suggests that the beam electrons first become trapped.

However, the beam electron transit time is comparable to the growth time of the field, so that the adiabatic approximation is not so good for them and may not be used for quantitative calculations. It does contain a germ of qualitative understanding of the initial nonlinear interation: The electric field grows until it is large enough to trap the beam electrons. As described more fully in Ref. 9, the trapping process is best visualized in terms of a sequence of diagrams of the electron $(x,\ v)$ phase space coordiates in the wave frame.

Initially, the beam electrons are distributed along the line $v=v_{0b}$. At the instant of marginal trapping, they will be distributed along an inverted u-shaped line in the upper $(v>0)$ half-plane of phase space, with some electrons just reduced to zero velocity in the wave frame. [If J invariance were valid, this beam electron trajectory would have the form $v=2(eE(t)/mk)^{1/2}|\cos kx|$.] This onset of a multivalued flow velocity $v(x)$ is a frame-invariant symptom of the trapping of a cold species. Subsequently, beam electrons will rotate into the lower $(v<0)$ half-plane of phase space, giving up a substantial amount of laboratory frame (i.e., the initial frame of the background electrons) kinetic energy to the background and field as they do so. After a half-cycle, beam electrons will be distributed along a u-shaped trajectory with negative wave frame velocities, and they will have given up a maximum amount of kinetic energy. At this point the electric field will be nonlinearly saturated, having achieved its maximum energy. As the beam particles continue to rotate in phase space through the second half-cycle, they retrieve some of the lost laboratory frame kinetic energy, and the electric field energy correspondingly decreases from its maximum to a relative minimum. Owing to the nonadiabaticity of the beam electrons, they are trapped on different energy contours, rotate at different frequencies, and hence become smeared out in phase space. This will cause the amplitude of the field energy fluctuations to decay, and the system therefore assumes the character of a metastable state with some mean field energy about which the decaying fluctuations occur.

Since the background electrons continue to obey linear theory, their laboratory frame kinetic ("sloshing") energy is equal to the electric field energy, and hence is half of the energy given up by the beam electrons. Therefore, one finds[10] that

$$\mathcal{E}_{\mathrm{mean}}\approx\tfrac{1}{2}\mathcal{E}_{\mathrm{max}}\approx\tfrac{1}{2}n_b mu(u-v_\varphi)\approx 2^{-4/3}\eta^{1/3}T_b(0), \quad (10)$$

where $\mathcal{E}_{\mathrm{max}}$ is the saturation energy, $\mathcal{E}_{\mathrm{mean}}$ is the electric field energy in the metastable state, and v_φ is the wave phase velocity, for which the linear value is used. Of course, the background electrons are still very much untrapped: $\kappa_e\gg 1$.

III. THE SINGLE WAVE BERNSTEIN–GREENE–KRUSKAL STATIONARY STATE

Since the result of the nonlinear dynamical theory is that the beam–plasma system seems to approach some sort of metastable state—except for possible long term effects—we address the question of whether or not there exists a Bernstein–Greene–Kruskal stationary state for which

(1) the electric field consists of a single sinusoidal mode,

(2) the beam electrons are completely trapped, and

(3) the total energy density, momentum density, and particle number density (of each species) are conserved with respect to the initial state of the cold, weak beam–plasma instability.

We do *not* prescribe *a priori* the wavenumber, the wave phase velocity (i.e., the frame in which the wave is stationary), or the amplitude of the electric field. The linear theory predictions of these quantities are found in Eqs. (6) and (10).

We proceed in the spirit of the original Bernstein–Greene–Kruskal paper of 1957.[11] The calculation is performed in the wave frame so that all quantities are time independent. The solutions to the time-independent Vlasov equation must be functions of $H(x, v)=\tfrac{1}{2}mv^2-(eE_\alpha/k_\alpha)\cos k_\alpha x$, where the electric field has the assumed form

$$E(x)=E_\alpha \sin k_\alpha x=-\frac{d\varphi(x)}{dx},$$

and

$$\varphi(x)=(E_\alpha/k_\alpha)\cos k_\alpha x.$$

The infinitely massive ions enter only in a trivial manner as usual. The distribution of the untrapped background electrons is assumed known—given by the approximation of adiabatic invariance, which agrees to several orders in $\eta^{1/3}$ with the approximation of linear theory. This distribution is given in Eqs. (11) and (12) below:

$$F_e(x, v)=F_e[H(x, v)]$$
$$=\pi n_e\left(\frac{meE_\alpha}{k_\alpha}\right)^{1/2}\kappa_e K^{-1}(\kappa_e^{-1})\delta(H-H_e), \quad (11)$$

$$\frac{4}{\pi}\left(\frac{eE_\alpha}{mk_\alpha}\right)^{1/2}\kappa_e E_2(\kappa_e^{-1})=u-v_{0b}=J_e. \quad (12)$$

Here, H_e and κ_e may be thought of as completely equivalent and interchangeable parameters, related though the definition $\kappa_e\equiv[\tfrac{1}{2}(1+k_\alpha H_e/eE_\alpha)]^{1/2}$. Either parameter may be replaced by the other via this definition, and we express the equations in terms of whichever parameter seems more convenient. The unknown quantity v_{0b} is the initial velocity of the beam electrons relative to the stationary wave frame. We note that the background electrons are hydrodynamically cold, being distributed along a constant energy (H_e) contour in phase space. The normalization factors in Eq. (11) have been chosen to satisfy Eq. (2) for conservation of background particles.

We proceed as in the Bernstein–Greene–Kruskal paper by inverting Poisson's equation to obtain the distribution of trapped beam electrons. It is convenient to employ the substitution

$$\int_{-\infty}^{\infty} dv\,\zeta(x, v)\to\int_{H(x,v=0)}^{\infty} dH\left(\frac{\zeta(H, x)}{(\partial H/\partial v)(H, x)}\right),$$

where $(\partial H/\partial v)(H, x)=mv(H, x)=\pm\{2m[H+e\varphi(x)]\}^{1/2}$. For the background electrons this procedure is unambiguous since they always have negative velocities (as can be verified later) and one need only be careful to keep the signs straight. The trapped beam electrons must be symmetrically distributed between the two directions of velocity in order to have a time-independent distribution. Therefore, a factor of 2 may occur in the mapping from v to H, but this factor is assumed absorbed in $\zeta(H, x)$.

We may now write equations which correspond to Eqs. (9), (10), and (11) of the Bernstein–Greene–Kruskal paper, and for convenience we adopt reasonably similar notation.

$$n_b(x)=g(e\varphi)$$
$$=\int_{-e\varphi}^{-e\varphi_{\min}} dH_b F_b(H_b)[2m(H_b+e\varphi)]^{-1/2} \quad (13)$$

is just the density of the trapped beam electrons. The implication of Eq. (13) that $g(e\varphi_{\min})=0$ simply reflects the fact that the beam particle density must vanish at the nodes of the trapping separatrix [i.e., at the points $x=\pm(\pi/k_\alpha)\times$odd integer]. One also notes that for the trapped beam electrons,

$$-e\varphi_{\max}=-eE_\alpha/k_\alpha\leq H_b\leq eE_\alpha/k_\alpha=-e\varphi_{\min},$$
$$\text{or}\quad 0\leq\kappa_b\leq 1.$$

Poisson's equation is invoked to determine the trapped beam particle density in terms of the known background density, ion density, and the electrostatic potential:

$$\begin{aligned}n_b(x)=g(e\varphi)&=\frac{1}{4\pi e}\frac{d^2\varphi}{dx^2}+n_e+n_b\\&\quad-\int_{-e\varphi_{\min}}^{\infty}dHF_e(H)[2m(H+e\varphi)]^{-1/2}\\&=-(k_\alpha^2/4\pi e^2)V+n_e+n_b-\pi n_e(eE_\alpha/2k_\alpha)^{1/2}\\&\quad\times\kappa_eK^{-1}(\kappa_e^{-1})(H_e+V)^{-1/2}=g(V),\quad(14)\end{aligned}$$

where $V\equiv e\varphi=(eE_\alpha/k_\alpha)\cos k_\alpha x$. With $g(e\varphi)$ determined from Eq. (14), one may invert Eq. (13) to obtain the distribution $F_b(H_b)$ of the trapped beam electrons. This may be done by noting that (13) is an integral equation of the convolution type and hence solvable by the Laplace transformation, or by noting that (13) has the form of Abel's equation whose solution is familiar. The result is

$$F_b(H_b)=\frac{(2m)^{1/2}}{\pi}\int_{e\varphi_{\min}}^{-H_b}dV\frac{dg(V)}{dV}(-H_b-V)^{-1/2}.\quad(15)$$

If Eq. (14) is inserted into (15), the integrations may be performed to yield

$$\begin{aligned}F_b(H_b)&=-(\tfrac{1}{2}m)^{1/2}\frac{k_\alpha^2}{\pi^2e^2}\left(\frac{eE_\alpha}{k_\alpha}-H_b\right)^{1/2}+n_e(\tfrac{1}{2}m)^{1/2}\\&\quad\times(1-\kappa_e^{-2})^{-1/2}K^{-1}(\kappa_e^{-1})\frac{[(eE_\alpha/k_\alpha)-H_b]^{1/2}}{H_e-H_b}.\quad(16)\end{aligned}$$

The solution for the beam particle density represented by Eq. (14) will automatically satisfy Eq. (2) for conservation of beam particles [i.e., $\langle n_b(x)\rangle=n_b$] since the coefficients in Eq. (11) were chosen to conserve background particles. However, the requirement that $g(e\varphi_{\min})=0$ is not automatically satisfied by Eq. (14), and so this condition replaces the particle conservation as a constraint among the various unknowns:

$$\begin{aligned}g(e\varphi_{\min})&=(k_\alpha E_\alpha/4\pi e)+n_e+n_b\\&\quad-\tfrac{1}{2}\pi n_e(1-\kappa_e^{-2})^{-1/2}K^{-1}(\kappa_e^{-1})=0.\quad(17)\end{aligned}$$

This equation may also be thought of as a boundary condition [to Eq. (13)], whose validity was tacitly assumed in the inversion of Eq. (13) to Eq. (15).

One now imposes the remaining constraints of Eqs. (3) and (4) for the conservation of the total momentum and energy density relative to the initial state of the cold, weak beam–plasma instability. Noting that the final state wave frame momentum of the beam electrons must vanish by symmetry, for the momentum conservation one obtains

$$\begin{aligned}&-\pi n_e\left(\frac{meE_\alpha}{k_\alpha}\right)^{1/2}\kappa_eK^{-1}(\kappa_e^{-1})\\&\qquad+mn_e(u-v_{0b})-mn_bv_{0b}=0.\quad(18)\end{aligned}$$

For energy conservation, one finds

$$\begin{aligned}&-\frac{E_\alpha^2}{32\pi}+\frac{\pi n_eeE_\alpha}{k_\alpha}(\kappa_e^2-\tfrac{3}{4})(1-\kappa_e^{-2})^{-1/2}K^{-1}(\kappa_e^{-1})\\&\qquad-\tfrac{1}{2}mn_e(u-v_{0b})^2-\tfrac{1}{2}mn_bv_{0b}^2=0.\quad(19)\end{aligned}$$

Now, the problem is reduced to an examination of the equations for consistent solutions. The background parameter κ_e (or H_e) is determined, in principle, by Eq. (12), and the remaining three parameters of the single wave Bernstein–Greene–Kruskal stationary state (k_α, v_{0b}, E_α) are determined from the constraint Eqs. (17), (18), and (19), provided that these equations have a consistent set of solutions. If one expands these equations in the small parameters $\eta^{1/3}\ll1$ and $\kappa_e^{-1}\ll1$, one finds that they do have unique consistent solutions, which are summarized below:

$$\begin{aligned}\kappa_e^{-1}&=2\eta^{1/3}(1+\tfrac{13}{24}\eta^{1/3}+\cdots),\\k_\alpha&=(\omega_p/u)(1+\tfrac{13}{8}\eta^{2/3}+\cdots),\\v_{0b}&=u-v_{\varphi\alpha}=\tfrac{1}{2}\eta^{1/3}u(1+\tfrac{5}{3}\eta^{1/3}+\cdots),\\\mathcal{E}_\alpha&=(16\pi)^{-1}E_\alpha^2=\tfrac{1}{2}\eta^{1/3}T_b(0)(1+\tfrac{1}{6}\eta^{1/3}+\cdots).\end{aligned}\quad(20)$$

It is interesting to compare these results with the linear theory predictions of Eqs. (6) and (10). One notes that k_α differs from k_L only by terms of $O(\eta^{2/3}k_L)$. Since the half-width of the $\gamma(k)$ function is $O(\eta^{1/3}k_L)$, the Bernstein–Greene–Kruskal wavenumber also falls right on the peak of $\gamma(k)$ as is to be expected. Comparison of the phase velocities reveals the significant fact that the Bernstein–Greene–Kruskal wave phase velocity is about $\frac{1}{10}\eta^{1/3}u$ slower than the linear phase velocity. Hence, as the system evolves toward the stationary state, the wave must be slowed by nonlinear effects. The predicted electric field energy of Eq. (10) is seen to be about 20% lower than the value found in Eq. (20). This is because the calculation of Eq. (10) did not anticipate the slowing of the wave. In light of this new information, it would be appropriate to increase the prediction of the maximum field energy from $2^{-1/3}\eta^{1/3}T_b(0)$ to some value between $2^{-1/3}\eta^{1/3}T_b(0)$ and $\eta^{1/3}T_b(0)$, depending upon the slowing achieved at the time of the first energy peak.

In the laboratory frame, the change in kinetic energy density which occurs between the initial state and the stationary state is found to be $\Delta T_{e\,\text{lab}}=\mathcal{E}_\alpha(1+\eta^{1/3}+\cdots)$ and $\Delta T_{b\,\text{lab}}=\mathcal{E}_\alpha(-2-\eta^{1/3}-\cdots)$, which confirms the splitting of beam energy between the background electrons and the field. In the wave frame, however, it is the background electrons which give up energy, most going to the electrostatic field and only $\eta^{1/3}\mathcal{E}_\alpha$ going to the beam. In the wave frame, the beam loses energy of directed motion in the amount $\frac{1}{2}mn_b v_{0b}^2 \approx \frac{1}{2}\eta^{1/3}\mathcal{E}_\alpha$ as it is slowed by the wave, but it gains thermal energy in the amount $\frac{3}{2}\eta^{1/3}\mathcal{E}_\alpha$ with the difference provided by the background electrons. This thermal energy corresponds to an average beam thermal velocity of $v_{b\theta} \approx \frac{1}{2}\sqrt{3}\eta^{1/3}u$.

One may examine, within linear theory, the effect of increasing the beam thermal velocity from zero (as treated herein) to a value high enough that the beam becomes a gentle bump (as treated by Drummond and Pines[1]). Such a transition analysis has been completed by O'Neil and Malmberg,[12] and reveals a nontrivial change in the topology of the dispersion relation when the thermal velocity of the beam is increased to $v_{b\theta} \sim \eta^{1/3}u$. Since nonlinear effects must eventually halt the growth of the cold beam–plasma instability, and since the trend from cold beams to warm beams to gentle bumps to quasilinearly flattened bumps is ever in the direction of increased stability, the implication is clearly that the nonlinear stabilization is likely to be accompanied by such effects as the heating of the beam to thermal velocities of $O(\eta^{1/3}u)$. We see that this inference is correct.

Consider briefly the Bernstein–Greene–Kruskal particle distribution. We have already remarked that the background electrons are hydrodynamically cold, being distributed along a constant energy contour as indicated by Eq. (11). However, their flow velocity has fluctuations of $O(\eta^{2/3}u)$. The spatially averaged distribution of the background particles in the wave frame is

$$\langle F_e[H(x,v)]\rangle \cong (mn_e u/\pi) \times[(eE_\alpha/k_\alpha)^2-(\tfrac{1}{2}mv^2-H_e)^2]^{-1/2}, \quad (21)$$

where

$$-\left[\frac{2}{m}\left(H_e+\frac{eE_\alpha}{k_\alpha}\right)\right]^{1/2} < v_{\text{background/wave frame}} < -\left[\frac{2}{m}\left(H_e-\frac{eE_\alpha}{k_\alpha}\right)\right]^{1/2}.$$

If these limits are expressed in the lab frame using the results of Eq. (20), one obtains

$$-\eta^{2/3}u < v_{\text{background/lab frame}} < \eta^{2/3}u. \quad (22)$$

For the beam electrons, one may expand Eq. (16) using the results of Eq. (20) to obtain

$$F_b(H_b) \cong \frac{2^{1/2}n_b}{\pi v_{0b}}\left(1-\frac{k_\alpha H_b}{eE_\alpha}\right)^{1/2}[1+O(\eta^{1/3})]. \quad (23)$$

It is appropriate to note that $F_b(H_b)$ is guaranteed the positive definite character so desirable to distribution functions, provided that $\eta^{1/3}$ is small enough. Also, the trapped beam electrons completely fill the region of phase space bounded by the trapping sepa-

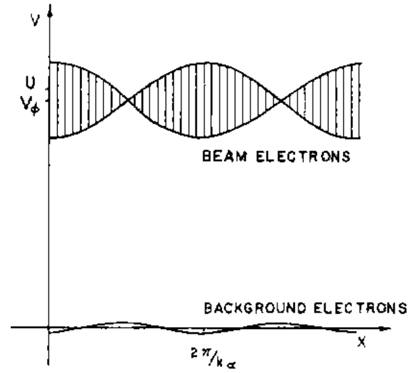

FIG. 2. Bernstein–Greene–Kruskal phase space diagram.

ratrix, rather than leaving unfilled holes in these regions. If one spatially averages the beam distribution of Eq. (23), one obtains

$$\langle F_b(H_b)\rangle = \frac{4n_b}{\pi^2 v_{0b}} Q\left[\left(1-\frac{k_\alpha mv^2}{4eE_\alpha}\right)^{1/2}\right], \quad (24)$$

where

$$Q(q) \equiv E_2(q)-(1-q^2)K(q)$$

and

$$|v_{\text{beam/wave frame}}| < 2(eE_\alpha/mk_\alpha)^{1/2} \approx 2\eta^{1/3}u \approx 4v_{0b}.$$

Therefore, in the laboratory frame

$$u(1-\tfrac{5}{2}\eta^{1/3}-\tfrac{11}{12}\eta^{2/3}) < v_{\text{beam/lab}} < u(1+\tfrac{3}{2}\eta^{1/3}-\tfrac{3}{4}\eta^{2/3}). \quad (25)$$

Comparing Eqs. (22) and (25) through $O(\eta^{2/3})u$ allows one to conclude that the beam electrons and background electrons will clearly be separated in phase space provided that $\eta^{1/3} \lesssim 0.32$. Of course, this is so in the limiting case of small $\eta^{1/3}$ in which our expansions are most respresentative of the truth. In Fig. 2, the occupied regions of phase space in the stationary state are indicated, and in Fig. 3 the Bernstein–Greene–Kruskal particle distributions of Eqs. (21) and (24) are illustrated.

It may be shown[13] that this Bernstein–Greene–Kruskal stationary state is also derivable without additional approximations from the warm hydrodynamical, or moment equations. This is possible because the energy and momentum conservation equations involve no moments higher than the pressure (i.e., the second moment), and the heat flow function vanishes identically for the beam particles to decouple the higher moment equations.

The stability of this stationary state has thus far been pursued rigorously only to the point of deriving an integral equation for the eigenmodes of the perturbed electric field.[14] Preliminary indications are that the only modes which retain a possibility of growth instability are precisely those short wavelength modes for which the inhomogeneity of the equilibrium cannot be swept aside.

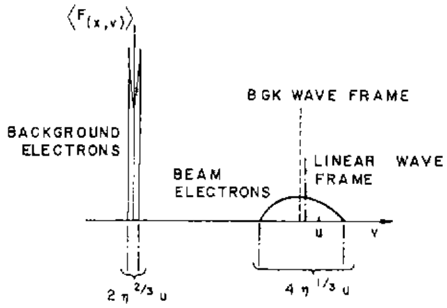

FIG. 3. Bernstein–Greene–Kruskal stationary state particle distributions.

In summary, the existence of a unique single wave Bernstein–Greene–Kruskal stationary state for the cold weak beam–plasma instability has been established. It has not been shown rigorously that the system does in fact evolve to this stationary state, but the circumstantial evidence suggests strongly that it at least comes very close. For example, the wavelength is in essential agreement with that which dominates the linear phase of evolution, the energy level is of the predicted order of magnitude, and the computer simulations of this problem reveal nonlinear trends toward this state such as the slowing of the wave below its linear phase velocity.

The question of the ultimate, time-asymptotic fate of this instability remains open. Whether or not the system approaches the stationary state, or merely oscillates about it several times before evolving in a different direction, will largely depend on the stability properties of the stationary state as well as on such long time effects as the decorrelation of the single mode spectrum and the gradual appearance of single particle or collisional effects.

IV. RESULTS OF COMPUTER CALCULATIONS

The nonlinear limit of beam–plasma instabilities has been studied by a number of people by computer simulation of the problem. Many of these studies have not applicable to the problem analyzed herein because the length separation stipulated in Eq. (1) (i.e., $2\pi u/\omega_{pe} \gg \lambda_{De}$) was not very wide, or because the "weakness" parameter $\eta^{1/3}$ was not so small. We now present the results of two calculations in which all assumptions were obeyed, for comparison with the theoretical results.

The first calculation was that of Nordsieck,[15] who considered the large signal behavior of traveling wave amplifiers, following the analysis by Pierce[16] and others on the small signal behavior. He began with the equations of motion of the electron stream, and with a circuit equation for the electric field. The circuit equation has the form of Kelvin's transmission-line equation, with the beam electrons treated as a distributed generator. From these equations, Nordsieck derived working equations [i.e., his Eqs. (13), (14), (17), and (20)] which were then solved numerically. His treatment was of a boundary value problem in space rather than an initial value problem in time.

However, it is possible to begin with Poisson's equation, and the equations of motion (which correspond to the Vlasov equation), and to derive therefrom the working equations of Nordsieck. In this derivation, one may consider an initial value problem in time, under the assumptions that $\eta^{1/3} \ll 1$, that the background electrons behave linearly, and that the electric field spectrum is dominated by a single wave. Thus, the background electrons correspond formally to the circuit of the traveling wave tube, and Nordsieck's results, which he presented graphically, may be reinterpreted as results for the weak beam–plasma instability. Nordsieck followed the problem to the first minimum beyond the initial maximum of the electrostatic field energy. The correspondence between Nordsieck's parameters and our own is summarized in Table I.

The second calculation was a computer simulation[17] in which the equations of motion of a large number (e.g., 4000) of electrons were iterated as they evolved in a self-consistent electric field. Poisson's equation was solved by the particle-in-cell method. To take advantage of the fact that background electrons react only linearly, they were "weighted" so that fewer (but heavier and more highly charged) background electrons need be followed on the computer. A value of $\eta \leq 10^{-3}$ was used, and typical values of the cell size, time step, and periodicity length are $\Delta x = 0.02(2\pi u/\omega_p)$, $\Delta t = 0.005(2\pi/\omega_p)$, $L = 4(2\pi u/\omega_p)$. Storage and time limitations dictate that the problem be box normalized on a relatively coarse scale, so that only a few modes occur within the growth curve $\gamma(k)$ of Fig. 1.

In both of the numerical calculations, it was not feasible to begin with a noisy perturbation of infinitesimal magnitude, and allow it to e-fold many (e.g., 20–30) times before the single mode structure was established and nonlinear saturation occurred. Instead one must establish a much larger perturbation which then e-folds only a moderate (e.g., 8–12) number of

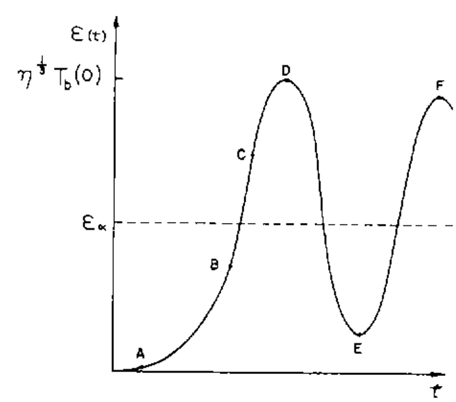

FIG. 4. Electric field energy vs time.

TABLE I. Correspondence between Nordsieck's notation and ours.

Nordsieck's notation	Present notation	
	Any single wave	Most unstable wave $\{k=(\omega_p/u)[1+O(\eta^{2/3})]\}$
u_0	u	
v_0	ω_p/k	$u[1-O(\eta^{2/3})]$
V_0/I_0	$2\pi u/\eta\omega_p^2$	
Z_0	$4\pi/k\omega_p$	$(4\pi u/\omega_p^2)[1-O(\eta^{2/3})]$
C^3	$\eta\omega_p/2ku$	$(\frac{1}{2}\eta)[1-O(\eta^{2/3})]$
b	$(2ku/\eta\omega_p)^{1/3}[1-(\omega_p/ku)]$	$O(\eta^{1/3})$
V_0	$mu^2/2e$	
y	$(\frac{1}{2}\eta)^{1/3}(ku/\omega_p)^{2/3}\omega_p t$	$(\frac{1}{2}\eta)^{1/3}\omega_p t[1+O(\eta^{2/3})]$
$A^2(y)$	$(\omega_p/ku)^{2/3}[\mathcal{E}(t)/(\frac{1}{2}\eta)^{1/3}T_b(0)]$	$[\mathcal{E}(t)/(\frac{1}{2}\eta)^{1/3}T_b(0)][1-O(\eta^{2/3})]$
$[\theta(y)/y]$	$-(2ku/\eta\omega_p)^{1/3}\{1-[v_\varphi(t)/u]\}$	$-(2/\eta)^{1/3}\{1-[v_\varphi(t)/u]\}[1+O(\eta^{2/3})]$
β	$-(2ku/\eta\omega_p)^{1/3}\{1-[v_{\varphi L}(k)/u]\}$	$-\frac{1}{2}[1+O(\eta^{1/3})]$
$[\Delta\theta(y)/y]$	$(2ku/\eta\omega_p)^{1/3}\{[v_{\varphi L}(k)-v_\varphi(k,t)]/u\}$	$(2/\eta)^{1/3}\{[v_{\varphi L}-v_\varphi(t)]/u\}[1+O(\eta^{2/3})]$

times in energy prior to saturation. One may begin with a very small initial thermal velocity (e.g., $v_\theta\leq 10^{-3}u$), or else with a small density perturbation (e.g., $\delta n\leq 10^{-2}n$), usually of the most unstable mode (only). The results are not particularly sensitive to the mode of initialization provided that the perturbations are as small as indicated.

Figure 4 illustrates the computed electrostatic field energy development.[18] Specific results of the numerical calculations are itemized and discussed below. Where two numerical results are listed, the first is that of Nordsieck.

(1) When the electric field energy has grown to $\mathcal{E}=0.01\mathcal{E}_{\max}$ (i.e., point A), the growth rate is observed to be $\gamma\approx(0.97,\ 0.97\pm0.01)\gamma_L$. Even in thermally initiated simulations, the fundamental mode (i.e., $k\cong\omega_p/u$) will have captured 99% of the field energy by this time.

(2) The field energy at the onset of trapping (i.e., point B), when the flow velocity of the beam electrons first becomes multivalued, is found to be $\mathcal{E}_{\text{trapped}}\approx(0.39,\ 0.31\pm0.02)\mathcal{E}_{\max}$. This is a bit higher than the estimated level [i.e., $0.20\eta^{1/3}T_b(0)$] at which linear theory would break down for the beam electrons. By this time of overtaking, the growth rate has decreased to $\gamma\approx(0.79\pm0.04)\lambda_L$.

(3) The maximum field energy (i.e., point D) is found to be $\mathcal{E}_{\max}\cong(1.09,\ 1.02\pm0.08)\eta^{1/3}T_b(0)$. This is to be compared with the prediction of $0.80\eta^{1/3}T_b(0)$ of Eq. (10), and with the increased prediction of $(0.80$ to $1.00)\eta^{1/3}T_b(0)$ as a result of the Bernstein–Greene–Kruskal calculation.

(4) The field energy at the first minimum (i.e., point E) is found to be $\mathcal{E}_{\min}\cong(0.14,\ 0.12\pm0.03)\mathcal{E}_{\max}$. The time between the first maximum and the first minimum is $\Delta t\cong(2.12,\ 1.87\pm0.04)\gamma_L^{-1}$.

(5) By the time of the first minimum, Nordsieck's results show that the phase velocity of the wave has decreased by $\Delta v_\varphi\cong-0.043\eta^{1/3}u$. This compares to an eventual expected decrease of $\Delta v_\varphi\cong-0.103\eta^{1/3}u$ according to the Bernstein–Greene–Kruskal calculation.

(6) The second maximum in the field energy is roughly $\mathcal{E}_{\max-2}\approx(0.95\pm0.15)\mathcal{E}_{\max}$, where uncertainty is due to the rapidly mounting truncation error.

(7) Throughout the period of Fig. 4 (except perhaps prior to point A), the fraction of energy in the fundamental mode exceeded 95%.

(8) The ratio between the kinetic energy of the background electrons and the electric field energy is found to be 1.1 ± 0.1, or $1+O(\eta^{1/3})$, throughout Fig. 4. This confirms the linear behavior of the background electrons, and demonstrates the splitting of beam energy between the background and the field.

(9) The computer simulation conserved particles exactly, and conserved momentum to within at least $10^{-6}mn_bu$. The truncation error was reflected in a lack of energy conservation, which was less than $0.05\mathcal{E}_{\max}$ prior to the first minimum but rose rapidly thereafter.

In addition to the numerical results reported above, the expected correlation between phase space dynamics and field energy fluctuation was observed in the computer simulation. In particular, the trapping and rotation of beam electrons in phase space occurred just as described in Sec. II and Ref. 9. Figure 5 illustrates the

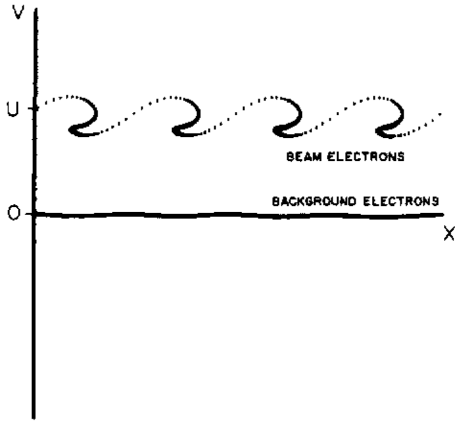

FIG. 5. Electron phase space coordinates.

phase space coordinates of electrons at a time corresponding to point C of Fig. 4, after trapping but before saturation of the field energy. The rotation of the trapped beam electrons is clearly indicated, and the linear sloshing of the background electrons may also be observed (barely).

In conclusion, the computer results agree quite nicely with one another and with the theoretical predictions. Unfortunately, the aforementioned truncation error and cost factors have precluded extending the computer calculations much beyond the domain of Fig. 4.

ACKNOWLEDGMENTS

The author is deeply indebted to Dr. W. E. Drummond and Dr. C. S. Gardner, whose generous guidance in this endeavor has been indispensable. Further thanks are due Mr. A. T. Drobot, who provided assistance in running the simulation code.

Financial support was provided by the National Defence Education Act and the University of Texas.

APPENDIX. ADIABATIC INVARIANCE

The approximation of adiabatic invariance which we have employed has been discussed extensively elsewhere,[19] and is a common procedure for dealing with periodic systems containing a parameter (e.g., the electric field amplitude) which varies only slowly in time. In such systems it may happen that on time scales long enough that some quantities (e.g., the Hamiltonian) vary appreciably, there are other quantities that vary negligibly and are hence said to be adiabatically invariant. Our adiabatic invariant is the familiar action integral: $J\sim\int p\,dq$.

The classical example of an adiabatic invariance problem is the harmonic oscillator (i.e., $H=\frac{1}{2}p^2+\frac{1}{2}\omega^2q^2$). When the frequency ω and hence the Hamiltonian H are slowly varying functions of time, their ratio will be adiabatically invariant.

Since the electric field amplitude changes slowly with respect to the dynamical time of transit of a background electron across a wavelength, this approximation of adiabatic invariance is appropriate for the background electrons and it may be shown[20] that for times shorter than $O(\eta\omega_p)^{-1}$, $J_{e\,\max}-J_{e\,\min}/J_e(t=0)\lesssim O(\eta)$. However, this is not as strong an endorsement of this approximation as may be made, since an "uncertainty" in the background electron velocity of $O(\eta u)$ would imply uncertainty in the momentum and energy density larger than that of the beam electrons, which would be intolerable. It is the case though that to the order required for the validity of the Bernstein–Greene–Kruskal calculation, J invariance is completely equivalent to linear theory for the background electrons; and linear theory is obviously justified since the ratio of the electric field energy density to the wave frame kinetic energy density of the background is $O(\eta^{4/3})$.

This equivalence is now illustrated via alternative calculations of the background particle density. We begin with a single wave linear theory calculation in the laboratory frame. If the electric field is taken to be $E(x,t)=E(t)\,\sin\Phi(x,t)$, where

$$E(t)=E_0\exp\int_0^t d\tau\gamma(\tau)$$

and

$$\Phi(x,t)=k\left(x-\int_0^t d\tau v_\varphi(\tau)\right),$$

then the background distribution function is found to be

$$F_e(x,v,t)=n_e\delta(v)+\frac{n_eeE(t)}{m}\left(\frac{k(v_\varphi-v)\cos\Phi+\gamma\sin\Phi}{k^2(v_\varphi-v)^2+\gamma^2}\right)\frac{\partial}{\partial v}\delta(v)+\cdots \quad \text{(A1)}$$

whence one obtains the density function

$$\frac{n_e(x,t)}{n_e}=1-\frac{eE(t)}{mkv_\varphi^2(t)}\cos\Phi(x,t)-\frac{2eE(t)\gamma(t)}{mk^2v_\varphi^3(t)}\sin\Phi(x,t)+\cdots. \quad \text{(A2)}$$

Here, we have allowed the growth rate and phase velocity to be slowly varying functions of time, but we have neglected the corrections involving $\dot\gamma(t)$, $\dot v_\varphi(t)$, etc. The last term listed in Eq. (A2) is $O(\eta)$ (i.e., the size of n_b/n_e) if one takes the linear growth rate, the Bernstein–Greene–Kruskal field amplitude, and any phase velocity of $O(u)$. However, as one approaches the stationary state, $\gamma(t)\to0$, $E(t)\to E_\alpha$, $v_\varphi(t)\to v_{\varphi\alpha}$, and hence the $\sin\Phi$ term in Eq. (A2) is eliminated.

The consideration of the transition between the initial state and the Bernstein–Greene–Kruskal stationary state via adiabatic invariance requires the construction of the adiabatically invariant series $J=J_0+J_1+J_2+$

$\cdots$, where the terms are of successively higher order in the slowness parameter. (Consideration of adiabatic invariance to higher orders in the slowness parameter is found in the previous work of Gardner[21] and Lenard,[22] among others.) For the background electrons, J_0 is given in Eq. (9) with $\kappa_e \gg 1$, and the next term is found to be

$$J_{1e}(\kappa_e, x, t) = [\gamma(t)/k](2/\pi)[E_2(\kappa_e^{-1})F(\kappa_e^{-1}, \tfrac{1}{2}kx) - K(\kappa_e^{-1})E_{2I}(\kappa_e^{-1}, \tfrac{1}{2}kx)]$$
$$= -\tfrac{1}{4}[\gamma(t)/k]\kappa_e^{-2}\sin kx + \cdots \quad \text{(A3)}$$

expressed in the instantaneous wave frame. (F and E_{2I} are incomplete elliptic integrals of the first and second kind.) The higher-order terms in the J series involve $\dot{\gamma}(t)$, $\dot{v}_\varphi(t)$, etc. and will not be needed. The J series must sum to the constant value $|v_{0e}|$, which is $v_\varphi(t)$ in the instantaneous wave frame. Because of the inclusion of the J_1 correction, the parameter κ_e has slight x dependence.

$$\kappa_e(x, t) = \frac{1}{2}\left(\frac{mk}{eE(t)}\right)^{1/2} v_\varphi(t) + \frac{1}{2}\left(\frac{eE(t)}{mk}\right)^{1/2}\frac{1}{v_\varphi(t)} + \frac{\gamma(t)}{kv_\varphi^2(t)}\left(\frac{eE(t)}{mk}\right)^{1/2}\sin kx + \cdots \quad \text{(A4)}$$

and so all particles no longer lie on the same constant energy contour. Instead, the contour on which the background electrons do lie cuts across a small spread of constant energy contours, and is given by

$$v(x, t) = -v_\varphi(t) - \frac{eE(t)}{mk}\frac{1}{v_\varphi(t)}\cos kx - \frac{eE(t)\gamma(t)}{mk^2v_\varphi^2(t)}\sin kx + \cdots. \quad \text{(A5)}$$

The density of such a string of electrons, which has deformed in phase space from the original line $v = -v_\varphi$ to the line of Eq. (A5), is simply

$$\frac{n_e(x, t)}{n_e} = -\frac{\partial v(x, t)}{\partial v_\varphi}$$
$$= 1 - \frac{eE(t)}{mkv_\varphi^2(t)}\cos kx - \frac{2eE(t)\gamma(t)}{mk^2v_\varphi^3(t)}\sin kx + \cdots \quad \text{(A6)}$$

which agrees exactly with the linear result of Eq. (A2). In a similar fashion, one may show that linear theory and J invariance yield identical results for the background momentum density $P_e(t)$ and the kinetic energy density $T_e(t)$ through terms the size of the beam momentum and energy density.

In relating the initial state of the system to a future stationary state, J invariance reduces to J_0 invariance since the higher-order terms in the J series vanish initially due to the infinitesimal electric field energy, and finally due to the vanishing slowness parameter.

* Present address: Austin Research Associates, Inc., Austin, Texas 78705.

† This work comprised a portion of the author's dissertation which was submitted in partial fulfillment of the requirements for the Ph.D. degree, University of Texas at Austin.

1 W. E. Drummond and D. Pines, Nucl. Fusion Suppl. Pt. 3, 1049 (1962).
2 A. A. Vedenov, E. P. Velikhov, and R. Z. Sagdeev, Nucl. Fusion Suppl. Pt. 2, 465 (1962).
3 D. W. Ross, Phys. Fluids **12**, 613 (1969).
4 K. V. Roberts and H. L. Berk, Phys. Rev. Letters **19**, 297 (1967).
5 R. L. Morse and C. W. Nielson, Phys. Rev. Letters **23**, 1087 (1969).
6 The problem of an ion beam-plasma interaction, with infinitely hot electrons which only provide gross charge neutrality is mathematically equivalent to this problem of an electron beam-plasma interaction with infinitely massive ions which only provide gross charge neutrality.
7 O. Buneman, Phys. Rev. **115**, 503 (1959).
8 One of many treatments of the linear theory is R. J. Briggs, *Electron-Stream Interactions with Plasmas* (MIT Press, Cambridge, Mass., 1964), Chaps. 2, 3.
9 W. E. Drummond, J. H. Malmberg, T. M. O'Neil, and J. R. Thompson, Phys. Fluids **13**, 2422 (1970).
10 Reference 9, see Eqs. (6) and (7).
11 I. B. Bernstein, J. M. Greene, and M. D. Kruskal, Phys. Rev. **108**, 546 (1957).
12 T. M. O'Neil and J. H. Malmberg, Phys. Fluids **11**, 1754 (1968).
13 J. R. Thomspon, Ph.D. thesis, University of Texas at Austin (1969), Chap. VI.
14 Reference 13, Chap. VII.
15 A. Nordsieck, Proc. IRE **41**, 630 (1953).
16 J. R. Pierce, Proc. IRE **35**, 11 (1947).
17 This was accomplished with a computer code obtained originally from R. L. Morse and C. W. Nielson, and subsequently modified somewhat.
18 See also Fig. 1 of Ref. 15.
19 A readable introduction may be found in L. D. Landau and E. M. Lifshitz, *Mechanics* (Pergamon, New York, 1960), Chap. 49.
20 Reference 13, Chap. IV.
21 C. S. Gardner, Phys. Rev. **115**, 791 (1959).
22 A. Lenard, Ann. Phys. (N.Y.) **6**, 261 (1959).